

Citation for published version:

E. Giacomidis, M. A. Jarajreh, S. Sygletos, S. T. Le, F. Farjady, A. Tsokanos, A. Hamié, E. Pincemin, Y. Jaouën, A. D. Ellis, and N. J. Doran, 'Dual-polarization multi-band optical OFDM transmission and transceiver limitations for up to 500 Gb/s uncompensated long-haul links', *Optics Express*, Vol. 22 (9): 10975-86, April 2014.

DOI:

<https://doi.org/10.1364/OE.22.010975>

Document Version:

This is the Published Version.

Copyright and Reuse:

© 2014 Optical Society of America.

Content in the UH Research Archive is made available for personal research, educational, and non-commercial purposes only. Unless otherwise stated, all content is protected by copyright, and in the absence of an open license, permissions for further re-use should be sought from the publisher, the author, or other copyright holder.

Enquiries

If you believe this document infringes copyright, please contact Research & Scholarly Communications at rsc@herts.ac.uk

Dual-polarization multi-band optical OFDM transmission and transceiver limitations for up to 500 Gb/s uncompensated long-haul links

E. Giacomidis,^{1,*} M. A. Jarajreh,² S. Sygletos,¹ S. T. Le,¹ F. Farjady,¹
A. Tsokanos,³ A. Hamić,⁴ E. Pincemin,⁵ Y. Jaouën,⁶ A. D. Ellis,¹ and N. J. Doran¹

¹Aston Institute of Photonic Technologies (AIPT), School of Engineering and Applied Science, Aston Triangle, Birmingham, B4 7ET, UK

²Faculty of Engineering & Environment, Northumbria University, Ellison Place, Newcastle upon Tyne, NE1 8ST, UK

³School of Computing and Mathematics, Plymouth University, B332, Portland Square, Drake Circus, Plymouth, UK

⁴Arts sciences and Technology University in Lebanon (AUL), P.O. Box: 14-6495 Beirut, Lebanon

⁵France Telecom - Orange Labs, 2 Avenue Pierre Marzin, 22307 Lannion, France

⁶Telecom-ParisTech, Département Communications & Électronique, 75013, 46 rue Barrault, Paris, France

*e.giacomidis@aston.ac.uk

Abstract: A number of critical issues for dual-polarization single- and multi-band optical orthogonal-frequency division multiplexing (DP-SB/MB-OFDM) signals are analyzed in dispersion compensation fiber (DCF)-free long-haul links. For the first time, different DP crosstalk removal techniques are compared, the maximum transmission-reach is investigated, and the impact of subcarrier number and high-level modulation formats are explored thoroughly. It is shown, for a bit-error-rate (BER) of 10^{-3} , 2000 km of quaternary phase-shift keying (QPSK) DP-MB-OFDM transmission is feasible. At high launched optical powers (LOP), maximum-likelihood decoding can extend the LOP of 40 Gb/s QPSK DP-SB-OFDM at 2000 km by 1.5 dB compared to zero-forcing. For a 100 Gb/s DP-MB-OFDM system, a high number of subcarriers contribute to improved BER but at the cost of digital signal processing computational complexity, whilst by adapting the cyclic prefix length the BER can be improved for a low number of subcarriers. In addition, when 16-quadrature amplitude modulation (16QAM) is employed the digital-to-analogue/analogue-to-digital converter (DAC/ADC) bandwidth is relaxed with a degraded BER; while the ‘circular’ 8QAM is slightly superior to its ‘rectangular’ form. Finally, the transmission of wavelength-division multiplexing DP-MB-OFDM and single-carrier DP-QPSK is experimentally compared for up to 500 Gb/s showing great potential and similar performance at 1000 km DCF-free G.652 line.

© 2014 Optical Society of America

OCIS codes: (060.0060) Fiber optics and optical communications; (060.2430) Fibers, single mode; (060.4080) Modulation; (060.1660) Coherent communications; (060.5060) Phase modulation;

References and links

1. S. L. Jansen, I. Morita, T. C. W. Schenk, N. Takeda, and H. Tanaka, “Coherent optical 25.8-Gb/s OFDM transmission over 4160-km SSMF,” *IEEE J. Lightw. Techn.* **26**(1), 6–15 (2008).
2. B. J. C. Schmidt, A. J. Lowery, and J. Armstrong, “Experimental demonstrations of 20 Gbit/s direct-detection optical OFDM and 12 Gbit/s with a colorless transmitter,” in *Proc. Opt. Fiber Commun. Conf., Anaheim, CA, 2007*, Paper PDP18.
3. S. C. J. Lee, F. Breyer, S. Randel, M. Schuster, J. Zeng, F. Huijskens, H. P. A. van den Boom, A. M. J. Koonen, and N. Hanik, “24-Gb/s transmission over 730 m of multimode fiber by direct modulation of an 850-nm VCSEL using discrete multi-tone modulation,” in *Proc. Opt. Fiber Commun. Conf., Anaheim, CA, 2007*, Paper PDP6.

4. W. Shieh, X. Yi, and Y. Tang, "Transmission experiment of multi-gigabit coherent optical OFDM systems over 1000 km SSMF fibre," *Electron. Lett.* **43**(3), 183–184 (2007).
5. S. L. Jansen, I. Morita, N. Takeda, and H. Tanaka, "20-Gb/s OFDM transmission over 4160-km SSMF enabled by RF-pilot tone phase noise compensation," in *Proc. Opt. Fiber Commun. Conf. (OFC)*, Anaheim, CA, 2007, Paper PDP 15.
6. S. L. Jansen, I. Morita, T. C. Schenk, and H. Tanaka, "121.9-Gb/s PDM-OFDM Transmission With 2-b/s/Hz Spectral Efficiency Over 1000 km of SSMF," *IEEE J. Lightw. Techn.* **27**(3), 177–188 (2009).
7. D. Qian, N. Cvijetic, J. Hu, and T. Wang, "40-Gb/s MIMO-OFDM-PON using polarization multiplexing and direct-detection," in *Proc. Opt. Fiber Commun. Conf.*, Anaheim, CA, 2009, Paper OMV 3.
8. Alcatel-Lucent, 1830 PSS brochure, www.alcatel-lucent.com Ciena 6500 product data sheet, www.ciena.com
9. H. Takahashi, S. L. Jansen, A. A. Amin, I. Morita, and H. Tanaka, "Comparison between Single-band and Multi-band optical OFDM at 120-Gb/s," in *Proc. Internat. Conf. on Opt. Internet (COIN 2008)*.
10. R. Dischler, F. Buchali, and A. Klekamp, "Demonstration of bite rate variable ROADM functionality on an optical OFDM superchannel," in *Proc. Opt. Fiber Commun. Conf. (OFC)*, 2010, Paper OTuM7.
11. T. Sakamoto, T. Kawanishi, and M. Izutsu, "Asymptotic formalism for ultraflat optical frequency comb generation using a Mach-Zehnder modulator," *Opt. Lett.* **32**(11), 1515–1517 (2007).
12. E. Giacomidis, J. Karaki, E. Pincemin, C. Gosset, R. Le Bidan, E. Awwad, and Y. Jaouën, "100 Gb/s coherent optical polarization multiplexed Multi-band-OFDM (MB-OFDM) transmission for long-haul applications," *International Conference on Transparent Optical Networks (ICTON)*, 2012, Paper We.B1.2.
13. J. Karaki, E. Giacomidis, D. Grot, T. Guilloisou, C. Gosset, R. Le Bidan, T. Le Gall, Y. Jaouën, and E. Pincemin, "Dual-polarization multi-band OFDM versus single-carrier DP-QPSK for 100 Gb/s long-haul WDM transmission over legacy infrastructure," *Opt. Express* **21**(14), 16982–16991 (2013).
14. J. Karaki, E. Pincemin, Y. Jaouën, and R. Le Bidan, "Frequency offset estimation in a Polarization-multiplexed coherent OFDM system stressed by chromatic dispersion and PMD," in *Proceedings of the Conference of Lasers and Electro-Optics (CLEO)*, (OSA, 2012), Paper CF1F.3.
15. K. Harako, D. Seya, T. Hirooka, and M. Nakazawa, "640 Gbaud (1.28 Tbit/s/ch) optical Nyquist pulse transmission over 525 km with substantial PMD tolerance," *Opt. Express* **21**(18), 21062–21075 (2013).
16. E. Giacomidis, J. L. Wei, X. L. Yang, A. Tsokanos, and J. M. Tang, "Adaptive modulation-enabled WDM impairment reduction in multi-channel optical OFDM transmission systems for next generation PONs," *IEEE Journal of Photonics* **2**(2), 130–140 (2010).
17. S. L. Jansen and I. Morita, "Polarization-division-multiplexed coherent optical OFDM transmission enabled by MIMO processing," *High Spectral Density Optical Communication Technologies, Optical and Fiber Communications Reports* **6**(2), 167–178 (2010).
18. W. Shieh, X. Yi, Y. Ma, and Q. Yang, "Coherent optical OFDM: has its time come?" [Invited], *IEEE/OSA J. Opt. Netw.* **7**(3), 324–355 (2008).
19. L. L. Hanzo, M. Munster, B. J. Choi, and T. Keller, *OFDM and MC-CDMA for Broadband Multi-User Communications, WLANs and Broadcasting* (Wiley-IEEE Press, 2003).
20. X. Q. Jin, J. L. Wei, R. P. Giddings, T. Quinlan, S. Walker, and J. M. Tang, "Experimental demonstrations and extensive comparisons of end-to-end real-time optical OFDM transceivers with adaptive bit and/or power loading," *IEEE Photonics Journal* **3**(3), 500–511 (2011).
21. S. Haykin, *Communication Systems*, 4th Ed. (Wiley & Sons Inc., 2001).
22. S. Chen, Q. Yang, Y. Ma, and W. Shieh, "Real-time multi-gigabit receiver for coherent optical MIMO-OFDM signals," *IEEE J. Lightw. Techn.* **27**(16), 3699–3704 (2009).

1. Introduction

Optical orthogonal frequency-division multiplexing (OFDM) is a very promising multi-carrier technique for long-haul transmissions [1] due to its high spectral efficiency and robust chromatic dispersion (CD) and polarization-mode dispersion (PMD) tolerance. Modern fiber-optic OFDM systems can be realized either with direct-detection optical (DDO) [2, 3] or with coherent optical (CO) detection [4, 5]. Using CO-OFDM in [6], a 121.9 Gb/s dual-polarization (DP) OFDM transmitted over 1000 km of standard single-mode fiber (SSMF) with 2 b/s/Hz spectral efficiency was demonstrated. DP CO-OFDM is preferred over DP DDO-OFDM not only due to its superior transmission performance but also due to the fact DP DDO-OFDM requires complex architectural design [7]. On the other hand, coherent DP quaternary phase-shift keying (DP-QPSK) is the current industrial solution for 100 Gb/s long-haul transport [8], whereas coherent DP multi-band OFDM (DP-MB-OFDM) [9] is a very interesting candidate for wavelength-division multiplexing (WDM) transmission at 400 Gb/s and up to 1 Tb/s.

Whilst DDO-OFDM is more suitable for cost-effective short-reach applications, the superior performance of CO-OFDM makes it an excellent candidate for long-haul

transmission systems. CO-OFDM is superior to DDO-OFDM in terms of spectral efficiency, simply because DDO-OFDM requires Hermitian symmetry [2]. In contrast to single-band (SB) OFDM, the employment of MB-OFDM significantly reduces the required digital-to-analogue/analogue-to-digital converter (DAC/ADC) bandwidth at comparable computational complexity [10]. Moreover, the confined and narrow spectrum of MB-OFDM makes it an ideal candidate for networks with many reconfigurable optical add-drop multiplexers (ROADMs). Another main advantage of MB-OFDM is its capability to optically switch at the sub-wavelength granularities thanks to the MB structure [11]. It should be noted that MB-OFDM approach is a pertinent alternative to single-carrier modulations providing similar transmission distances and offering natural rectangular spectrum [12–14]. In contrast to Nyquist-WDM [15], MB-OFDM technology does not require complex digital signal processing (DSP) to mitigate signal distortion induced by the transceivers filtering and additionally the ROADM cascading is more efficient.

The main constraint of OFDM signals in long-haul transmission is the fiber nonlinearity which considerably limits its transmission capacity (it might not be as efficient as single-carrier QPSK) due to the high peak-to-average power ratio (PAPR). After having answered to the aforementioned statement in [12–14], where it was shown that 100 Gb/s DP-MB-OFDM and single-carrier DP-QPSK have nearly the same performance after 10×100 km of G.652 fiber; here, we thoroughly explore the DP-MB-OFDM transmission and transceiver limitations to maximize performance. This paper addresses for the first time the following issues:

- Extensive investigation of the two dominant DP crosstalk removal techniques in high-speed communications: the zero-forcing (ZF) and maximum-likelihood (ML).
- Exploration of maximum transmission distance of 100 Gb/s DP-MB-OFDM (beyond the 1000 km exploration limit reported in [12]).
- Optimization of the OFDM subcarrier number to improve system performance.
- Investigation of high-level signal modulation formats impact on 100 Gb/s DP-MB-OFDM transmission.

Additionally, a comparison is also made between DP-MB-OFDM and the industrial solution of single-carrier DP-QPSK (with 25 GBaud symbol rate) [8] in WDM configuration for 500 Gb/s after 10×100 km dispersion compensation fiber (DCF)-free G.652 fiber line. Finally, we also focus on the theoretical aspects of multiple-input multiple-output (MIMO) equalization methods.

It is shown for a target bit-error-rate (BER) of 10^{-3} , 2000 km QPSK coherent DP-MB-OFDM of transmission is feasible. At relatively high launched optical powers (LOP), the strong nonlinear effects degrade the ZF technique and hence, ML decoding can enhance the DP OFDM transmission performance (1.5 dB of LOP extension compared to ZF). Investigations on the number of OFDM subcarriers indicate that a high number contributes to improved BER, while when *different* CP length is used, for a low number of subcarriers the BER is superior compared to the case of using *similar* CP length. By adopting a high signal modulation format (i.e. 16 quadrature amplitude modulation [16QAM]), the DAC/ADC bandwidth is relaxed with the cost of BER degradation; whereas the ‘circular’ 8QAM is slightly superior to its ‘rectangular’ form. Finally, it is experimentally revealed and numerically verified that 500 Gb/s WDM DP-MB-OFDM and WDM single-carrier DP-QPSK have similar transmission performance at 1000 km DCF-free G.652 fiber line.

2. Transceiver parameters and experimental set-up

In this Section, the DP-MB-OFDM transceiver parameters and experimental set-up are presented. For the numerical investigations, the developed OFDM transceivers as well as the optical transmission was implemented in a Matlab/VPI-transmission-Maker® co-simulated

environment (electrical domain in Matlab and optical components with SSMF in VPI). It should be noted that, phase noise and frequency offset has been considered in all the theoretical models developed in this paper. The DAC/ADC clipping ratio and quantization have been taken into account and set to 13 dB and 10-bits, respectively, which have no impact on the performance of OFDM signals for subcarrier number >32 [12, 14, 16]. Similar observations occur when no DAC/ADC clipping ratio and quantization bits are considered [12, 14, 16]. The DP-MB-OFDM system is generated by four OFDM sub-bands per polarization. The generated pseudo-binary random sequence (PBRBS) counts $2^{19}-1$ bits sent over 1000 symbols for 256 subcarriers per sub-band (169 are the data subcarriers and the rest 87 are the zero subcarriers) and an average BER is calculated for the four sub-bands. The nominal bit-rate of 100 Gb/s, increased up to 124.4 Gb/s after including the 7% overhead required for forward-error correction (FEC), the 7.03% for cyclic prefix (CP), the 6% for training symbols and the 2.3% for pilot tones, is split between the four polarization-multiplexed OFDM sub-bands. Each sub-band carries 31.1 Gb/s in a bandwidth of ~ 8 GHz while the sub-band spacing is 10 GHz. For the in-line optical amplification, an Erbium-doped fiber amplifier (EDFA) was adopted having 20 dB gain (G) and 5.5 dB noise figure (NF). The adopted SSMF parameters in this paper are the following: fiber nonlinear Kerr parameter, CD, CD-slope, fiber loss, and PMD coefficient of $1.1 \text{ W}^{-1}\text{km}^{-1}$, 16 ps/nm/km, 0.06 ps/km/nm², 0.2 dB/km and $0.1 \text{ ps/km}^{0.5}$, respectively. It should be noted that the transceivers parameters of DP-MB-OFDM are similarly to those described in [12–14]. The DP-MB-OFDM transceiver parameters are summarized on Table 1.

Table 1. DP-MB-OFDM transceiver parameters

Symbol	Description	Value	Unit
N_s	Number of OFDM subcarriers per sub-band	169	—
CP	Cyclic Prefix length	7.03	%
FEC	Forward-Error Correction	7	%
—	Max. SSMF transmission distance	2000	km
F_s	Sampling rate per sub-band	8	GHz
—	Signal bit-rate per sub-band	31.1	Gb/s
—	Nominal bit-rate	100	Gb/s
NF	EDFA Noise Figure	5.5	dB
G	EDFA Gain	20	dB
—	SSMF Span length	100	km
BPF	Band-Pass Filter	40	GHz
—	DAC/ADC Clipping Ratio	13	dB
—	DAC/ADC Quantization	10	bits
—	Training sequence for MIMO equalization	60	symbols
—	Pilot tones	2.3	%
—	OFDM sub-band spacing	10	GHz
—	WDM spacing	50	GHz
PRBS	Pseudo-Random Binary Sequence per OFDM sub-band	$2^{19}-1$	bits

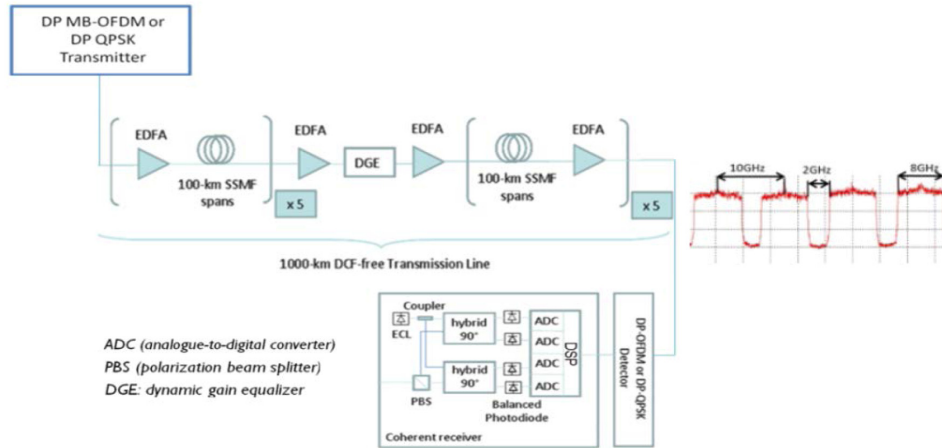


Fig. 1. Experimental DP-MB-OFDM and single-carrier DP-QPSK (at 25 GBaud) transmission-link diagram. Inset: 100 Gb/s DP-MB-OFDM spectra (x-polarization only shown here).

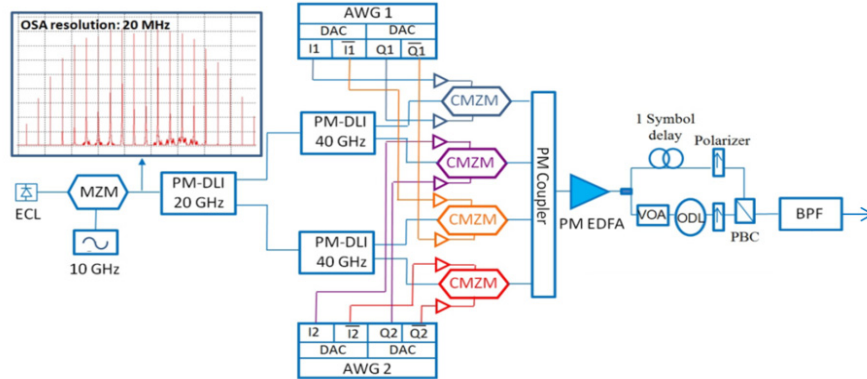


Fig. 2. Set-up of the 100 Gb/s DP-MB-OFDM transmitter with PBC (polarization beam combiner), OD (optical delay line), VOA (variable optical attenuator). Inset: Spectrum of the 10 GHz-spaced optical carriers at the MZM output.

For the experimental measurements, the electrical spectra (for x-polarization) of the four sub-bands at a total signal bit-rate of 100 Gb/s is depicted in the inset of Fig. 1. In addition, for both DP-MB-OFDM and single-carrier DP-QPSK, a DCF-free transmission line constituted by 10 spans of 100 km of G.652 SSMF was implemented as shown in Fig. 1. In the middle of the transmission line, a dynamic gain equalizer (DGE) was inserted in order to flatten the multiplex power after 1000 km. Figure 2 shows the experimental set-up of the employed 100 Gb/s DP-MB-OFDM transmitter. A comb of optical carriers spaced by 10 GHz (shown in the inset of Fig. 2) is generated by using an external cavity laser (ECL) and driving a dual-arm MZM with a 10 GHz RF. The required four optical carriers are selected at the transmitter output by a square flat-top optical band-pass filter (BPF) of ~ 40 GHz bandwidth. Before that, a combination of 20 GHz and 40 GHz polarization-maintaining delay line interferometers (PM-DLI) splits into four groups of carriers spaced by 40 GHz the initial comb of 10 GHz-spaced optical carriers. Each of the four generated combs is modulated by a complex-MZM (CMZM) and combined by a 4:1 polarization-maintaining (PM) coupler. The details over the generation and detection of the DP-MB-OFDM and single-carrier DP-QPSK signals, as well as the experimental set-up, are given in [12, 13]. In Table 1, the DP-MB-OFDM transceiver parameters are summarized.

3. MIMO processing

For the MIMO channel estimation of the developed DP-MB-OFDM system, the proposed MIMO equalizers of [17] for OFDM are adopted here. For a perfectly synchronized system, the received signal before MIMO processing $y(k)$ of the k -th subcarrier can be expressed as:

$$y(k) = H(k)s(k) + n(k) \quad (1)$$

where

$$H(k) = \begin{pmatrix} h_{11} & h_{12} \\ h_{21} & h_{22} \end{pmatrix} \quad (2)$$

represents the 2×2 channel matrix (Jones matrix) and vector $n(k)$ represents the frequency-domain noise within subcarrier k for the two received polarizations.

3.1 Zero-Forcing (ZF) equalization

The estimation of the transmitted stream after ZF processing is:

$$\tilde{s}(k) = \tilde{H}^+ + y(k) \quad (3)$$

where superscript denotes the pseudo-inverse operation, defined for a matrix A as

$$A^+ = (A^H A)^{-1} A^H \quad (4)$$

Here, H and -1 denote the conjugate transpose and matrix inverse, respectively. Assuming perfect channel estimation i.e., $\tilde{H}^+(k) = H^+(k)$, Eq. (3) can be written as

$$\tilde{s} = s(k) + H^+(k)n(k) \quad (5)$$

3.2 Maximum likelihood (ML) decoding

More advanced MIMO detectors have been employed to improve the performance in MIMO detection, such as ML estimation. If y denotes the received symbols, \tilde{H} the channel, \hat{x} the estimated symbols, and \bar{X} all symbols, then:

$$\hat{x} = \arg \min_x -\|y - \tilde{H} \bar{X}\| \quad (6)$$

However, this performance improvement comes at the cost of a significant increase in digital signal processing (DSP) computational complexity.

It should be noted that for the MIMO processing to work, the estimation of the MIMO channel in the receiver and the subcarrier recovery for phase estimation are similar to these described in [17, 18].

4. Comparison of MIMO equalization techniques: ZF versus ML

In this Section, the aforementioned MIMO equalization techniques of ZF and ML are compared in simple single-band configuration i.e. DP-SB-OFDM for the purpose of isolating the impact of the sub-bands crosstalk effects. For the DP-SB-OFDM numerical analysis, 2000 km of transmission is considered using QPSK at 40 Gb/s (20 Gb/s per polarization) employing 256 subcarriers at a sampling rate of 12 GS/s; and 20 spans of 100 km incorporating inline EDFA amplification are taken into account. In Fig. 3(a), the BER versus total input power ($P_{\text{IN SPAN}}$) per span is depicted for ZF and ML. It is shown, that the difference between ZF and ML is up to 0.5 dB (for low $P_{\text{IN SPAN}}$) and up to 1.5 dB (for higher

$P_{IN\ SPAN}$) around the BER of 10^{-3} (FEC-limit). At relatively high LOP the strong nonlinear effects degrade the ZF coding and hence, ML is a more feasible solution.

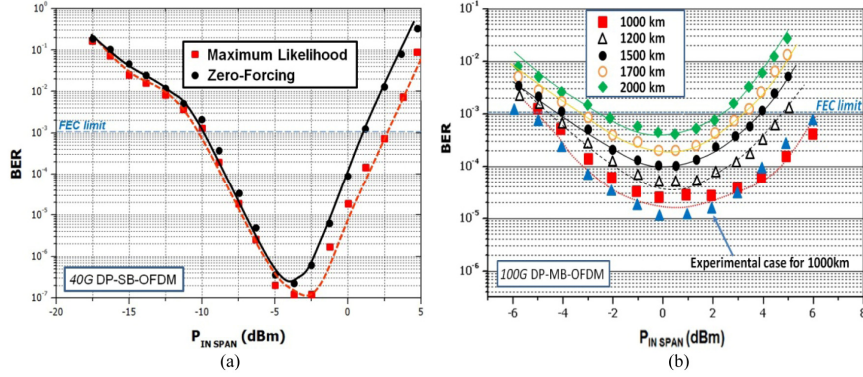


Fig. 3. (a) BER vs. $P_{IN\ SPAN}$: Transmission performance of 40 Gb/s QPSK DP-SB-OFDM for 2000 km using ZF and ML. (b) BER vs. $P_{IN\ SPAN}$: Transmission performance of 100 Gb/s QPSK DP-MB-OFDM over different distances.

5. Transmission distance limitations and subcarrier impact investigations

The transmission distance limitations are explored here for the developed 100 Gb/s DP-MB-OFDM. From Fig. 3(b), it is evident that for a BER of 10^{-3} , a transmission of 2000 km is feasible. It should be also noted that the experimental case for 1000 km (blue triangles) agree very well with the theoretical predictions confirming the validity of our developed numerical model.

Furthermore, the impact of subcarrier number on the transmission performance of the 100 Gb/s DP-MB-OFDM system is investigated in Figs. 4-5. The generated subcarrier number varies from 64 up to 512. From Fig. 4(a), it is shown that when the number of subcarriers is increasing the BER is reduced. This can be explained as follows: For a small number of subcarriers, the 7.03% CP length is relatively short. On the other hand, for a large number of subcarriers the CP length is sufficiently long, which can combat more effectively the CD effect, thus, the signal-to-noise (SNR) variation between subcarriers begins to play a role in determining the system performance.

In Fig. 4(b), the CP length is changing for different subcarrier number (in contrast to Fig. 4(a)) according to Eq. (7), in which the time T_g required to eliminate all inter-subcarrier interference (ISI) caused by CD and differential group-delay (DGD) can be expressed as,

$$\frac{c}{f_c^2} |D| N_s \Delta f + DGD_{\max} \leq T_g \quad (7)$$

where f_c is the optical carrier frequency, c is the speed of light, D is the total amount of CD, DGD_{\max} is the maximum budgeted DGD, N_s is the number of subcarriers, and Δf is the subcarrier frequency spacing. The DGD_{\max} has been approximately calculated to be ~ 3.5 times the mean PMD in typical fiber installations and that equals the OFDM symbol length in samples (excluding CP) [19]. In Fig. 4(b), for low number of subcarriers the BER is slightly improved compared to the case of Fig. 4(a). This happens because in Fig. 4(a), even if the CP length has been chosen to be long enough to virtually compensate for CD and PMD, the imperfect pilot-assisted phase estimation for low number of subcarriers contributes to a degraded BER. The last statement is confirmed in [19]. In Fig. 5, a BER vs. subcarrier number plot is depicted at optimum 1 dBm LOP ($P_{IN\ SPAN}$) for *similar* (7.03%) and *different* CP length after 1000 km of 100 Gb/s DP-MB-OFDM transmission, revealing the

performance improvement when using *different* CP length especially on low subcarrier number (e.g. 64 subcarriers).

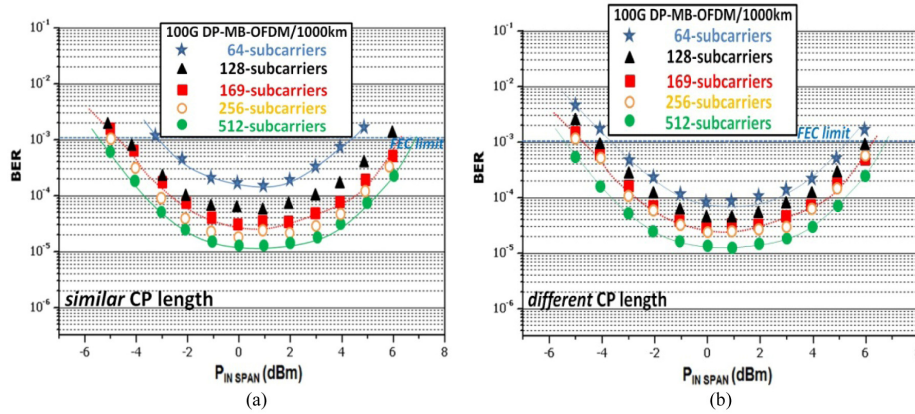


Fig. 4. (a) BER vs. $P_{IN\ SPAN}$: Transmission performance of 100 Gb/s DP-MB-OFDM using different subcarrier number with *similar* CP length (7.03%) after 1000 km. (b) BER vs. $P_{IN\ SPAN}$: Transmission performance of 100 Gb/s DP-MB-OFDM using different subcarrier number with *different* CP length after 1000 km.

At this point, it should be noted that even when adopting a high number of subcarriers (for example 512) the BER might have its minimum value; this increases complexity for implementation in real-time DSP Altera Stratix-II GX field-programmable gate array (FPGA)-based optical OFDM transceivers [20]. The lowest subcarrier number has the lowest level of resource usage across all key elements including combinational adaptive look-up tables (ALUTs), adaptive logic modules (ALMs), dedicated logic registers, block memory bits, and DSP block 9-bit elements [20]. Moreover, the lower complexity in resource usage results in significant reduction in manufacturing costs. Given the fact that the DSP resource usage is proportional to the number of adopted information bearing subcarriers, therefore, 169 subcarriers are always preferred to 512.

$$E_{av} = \frac{2(M-1)E_o}{3} \quad (8)$$

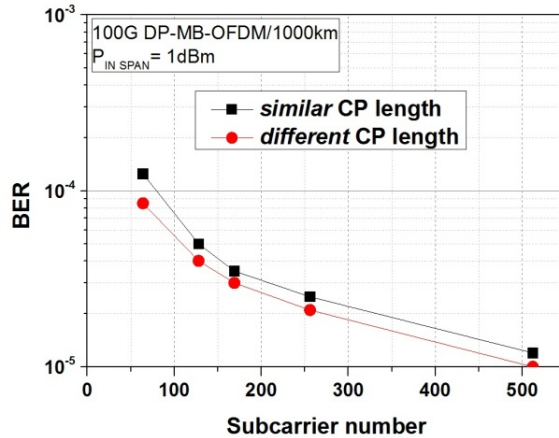


Fig. 5. BER vs. subcarrier number: Performance comparison of 100 Gb/s DP-MB-OFDM using different subcarrier number with *similar* (7.03%) and *different* CP length after 1000 km at 1 dBm LOP ($P_{IN\ SPAN}$).

5. Exploration of high-level signal modulation formats

In this Section, the impact of higher signal modulation formats than QPSK in the transmission performance of the 100 Gb/s DP-MB-OFDM is investigated. For achieving 100 Gb/s in the DP-MB-OFDM system using 16QAM and 8QAM, the DAC/ADC sampling rate per sub-band is adjusted to 4 GS/s and 5.35 GS/s, respectively. It should be noted that the sub-band spacing is maintained at 10 GHz. In Fig. 6(a), a schematic diagram of the 100 Gb/s DP-MB-OFDM system using 16QAM (OFDM sub-band sampling rate of 4 GS/s) is shown. In addition, for fair comparisons between different signal modulation formats the average energy per bit (E_{av}) is kept constant [21]. The E_{av} is expressed in Eq. (8), in which M is the signal modulation format level, and E_o is the energy per baud of the signal with the lowest amplitude.

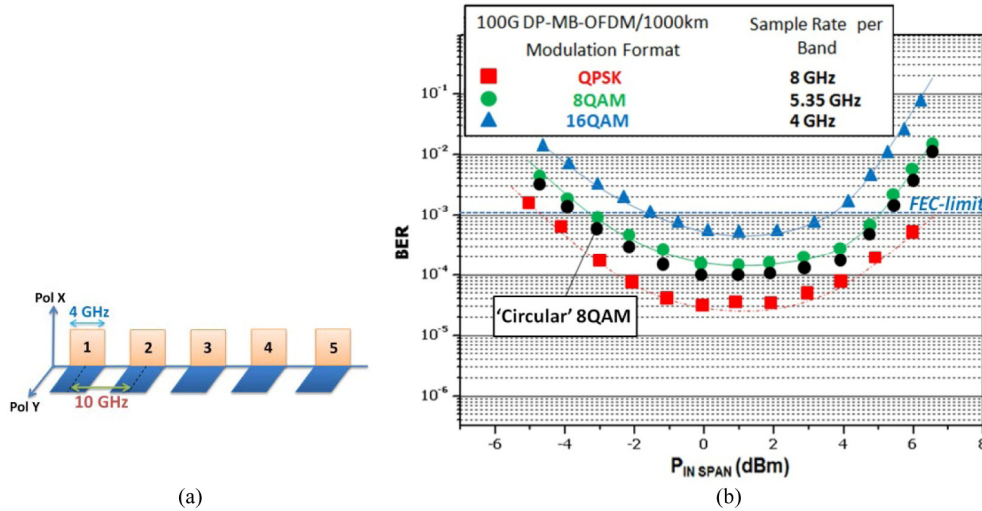


Fig. 6. (a) Schematic diagram of 100 Gb/s DP-MB-OFDM using 16QAM with OFDM sub-band sampling rate of 4 GHz. (b) BER vs. $P_{IN SPAN}$: Transmission performance comparisons of 100 Gb/s DP-MB-OFDM for different signal modulation formats, namely QPSK, 8QAM, 'circular' 8QAM and 16QAM for 1000 km.

In Fig. 6(b), a transmission performance comparison is made between different signal modulation formats, namely, QPSK, 8QAM and 16QAM over 1000 km. In addition, the 'circular' 8QAM is also compared with its 'rectangular' form. The corresponding received "corrected" constellation diagrams for 8QAM ('rectangular' and 'circular' with BERs of 2.2×10^{-3} and 9.0×10^{-5} , respectively), and 16QAM (BER of 10^{-3}) for x-polarization are depicted in Figs. 7-8. It is shown that the highest signal modulation format has the worst performance over the entire range of LOP of interest. This happens because when 16QAM is used for example, there are 4 bits/symbol and the threshold between constellation points is very small and hence more sensitive to errors in comparison to lower signal modulation formats. In addition, the BER for 16QAM is attributed to the large phase drift due to long OFDM symbol length by using relatively low sampling rate. The advantage of using higher signal modulation formats is the relaxation on the requirement of the DACs/ADCs bandwidth.

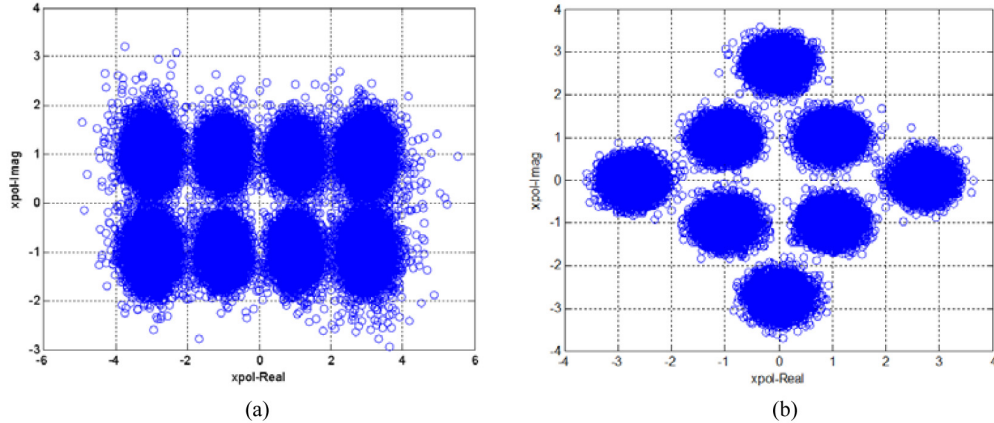


Fig. 7. Received 'corrected' constellation diagram of (a) 'rectangular' 8QAM and (b) 'circular' 8QAM for x-polarization with BERs of 2.2×10^{-3} and 9.0×10^{-3} , respectively.

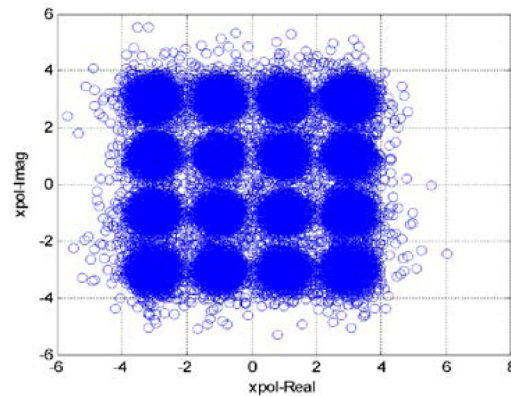


Fig. 8. Received 'corrected' constellation diagram of 16QAM for x-polarization with BER of 10^{-3} .

6. WDM DP-MB-OFDM versus WDM single-carrier DP-QPSK

Having explored the transmission performance of DP-MB-OFDM in single-channel (SC) configuration, here we present WDM transmission of DP-MB-OFDM and compare it with WDM DP-QPSK (experimental measurements with numerical verifications) for 500 Gb/s at 1000 km. For the WDM DP-MB-OFDM and single-carrier QPSK, five 50 GHz spaced wavelengths are generated with each one being modulated at 100 Gb/s using QPSK. The first WDM channel is modulated at 1552.524 nm. In Fig. 9, results from the worst-case middle WDM channel (3rd) are shown. For comparisons purposes, SC transmission of 100 Gb/s DP-MB-OFDM and 100 Gb/s single-carrier DP-QPSK are presented.

As revealed from Fig. 9, in such realistic conditions, WDM DP-MB-OFDM has nearly the same performance with WDM single-carrier DP-QPSK at 1000 km of transmission. Furthermore, as expected, the WDM signals have slightly more degraded BER than SC signals because the WDM crosstalk impairments of four-wave mixing (FWM) and cross-phase modulation (XPM) are dominant even at 50 GHz channel spacing. In addition, it is confirmed that SC 100 Gb/s DP-MB-OFDM and DP-QPSK have also nearly the same performance. Finally, it is worth mentioning that experimental measurements almost match with numerical predictions, confirming the validity of our numerical models.

In Table 2 results are summarized: The BER at optimum 1 dBm LOP is measured for different modulation type (single-carrier DP-QPSK, QPSK DP-MB-OFDM, and “rectangular” or “circular” 8QAM DP-MB-OFDM), signal bit-rate (up to 500 Gb/s) when considering single- and multi-channel systems.

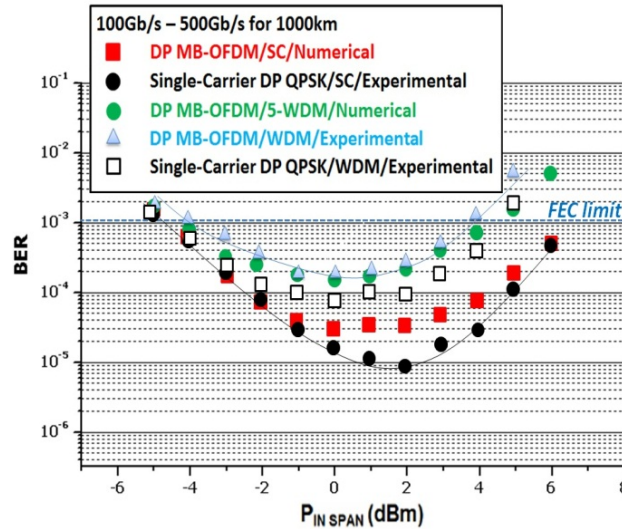


Fig. 9. BER vs. $P_{IN SPAN}$: Transmission performance comparisons of 100 Gb/s single-channel (SC) DP-MB-OFDM and single-carrier DP-QPSK, 500 Gb/s multi-channel (WDM) DP-MB-OFDM and single-carrier DP-QPSK (experimental results and numerical predictions at 1000 km): For the case of WDM configuration worst-case middle channel (3rd) is considered.

Table 2. BER performance for different modulation type and signal bit-rate at 1 dBm LOP when considering single- and multi-channels

Modulation Type	Number of Channels	Signal Bit-Rate	BER at 1 dBm LOP
Single-Carrier DP-QPSK	Single-Channel	100G	$1.2e^{-5}$
Single-Carrier DP-QPSK	4 Channels	400G	$1e^{-4}$
QPSK DP-MB-OFDM	Single-Channel	100G	$2e^{-5}$
QPSK DP-MB-OFDM	4 Channels	400G	$1.9e^{-4}$
QPSK DP-MB-OFDM	5 Channels	500G	$1.85e^{-4}$
QPSK DP-MB-OFDM	Single-Channel	100G	$3.5e^{-5}$
“rectangular” 8QAM DP-MB-OFDM	Single-Channel	100G	$1.5e^{-4}$
“circular” 8QAM DP-MB-OFDM	Single-Channel	100G	$1e^{-4}$
16QAM DP-MB-OFDM	Single-Channel	100G	$5e^{-4}$

LOP: Launched Optical Power

7. Conclusion

It was shown, for a target BER of 10^{-3} (FEC-limit), 2000 km of QPSK coherent DP-MB-OFDM transmission was feasible. It was revealed that for 40 Gb/s QPSK DP-SB-OFDM at 2000 km for relatively high LOP the strong nonlinear effects degrade the ZF polarization crosstalk removal technique by 1.5 dB compared to ML decoding. Investigations using different number of OFDM subcarriers indicated that a high number contribute to improved BER but at the cost of DSP computational complexity, while by using *different* CP length, for a low number of subcarriers the BER was superior compared to the case of using *similar* CP length. When higher signal modulation formats were adopted such as 16QAM, the DAC/ADC bandwidth was relaxed but the BER was degraded; whereas the ‘circular’ 8QAM was slightly superior to its ‘rectangular’ form. Moreover, the transmission of WDM DP-MB-

OFDM and single-carrier DP-QPSK has been experimentally and numerically compared at a total signal bit-rate of 500 Gb/s, showing great potential and similar performance for 1000 km DCF-free fiber line.

It should be mentioned, that, agreement between our theoretical investigations and experimental measurements has confirmed the validity of our numerical models. Finally, we have also focused on the theoretical aspects of MIMO equalization methods.

Acknowledgments

This work was supported by the EU FP7 projects DISCUS (Grant Agreement 318137) and FOX-C (Grant Agreement 318415), the EPSRC project UNLOC (Grant Agreement EP/J017582/1), the FUI9 100G-FLEX project of the “Pôle de Compétitivité Images & Réseaux”, and Aston Institute of Photonic Technologies (AIPT) for supporting the publication fee.